https://doi.org/10.5194/egusphere-2024-2930
Preprint. Discussion started: 20 November 2024

High-resolution air quality maps for Bucharest using Mixed-Effects Modeling Framework

Camelia Talianu[1,2,*], Jeni Vasilescu[1,*], Doina Nicolae[1,*], Alexandru Ilie[1,3], Andrei Dandocsi[1,4], Anca Nemuc[1], and Livio Belegante[1]

[1]National Institute of Research and Development for Optoelectronics-INOE 2000, Str. Atomistilor 409, Măgurele, 077125, Ilfov, Romania
[2]Institute of Meteorology and Climatology, Department of Water, Atmosphere and Environment, University of Natural Resources and Life Sciences, Gregor-Mendel Street 33, Vienna, A-1180, Vienna, Austria
[3]Faculty of Geography, University of Bucharest, Bulevardul Nicolae Bălcescu 1, Bucharest, 010041, Bucharest, Romania
[4]UNST Politehnica of Bucharest, Bulevardul Iuliu Maniu 1-3, Bucharest, 061071, Bucharest, Romania
[*]These authors contributed equally to this work.

Correspondence: Camelia Talianu (camelia@inoe.ro), Jeni Vasilescu (jeni@inoe.ro), and Doina Nicolae (nnicol@inoe.ro)

Abstract. Fine-scale mapping of pollutants based on mobile observations facilitates deep understanding of air pollutants distribution within a city and fosters science-based decisions to improve air quality, by adding up to the existing but not optimally distributed permanent monitoring stations. In this study, we developed high-resolution concentration maps of nitrogen dioxide (NO_2), particulate matter (PM_{10}) and ultrafine particles (UFP) for Bucharest, Romania, to evaluate the spatial variation of pollutants across the city during the warm and the cold seasons. Maps were generated using a mixed-effect method applied to a Land-use Regression (LUR) model. The approach relies on multiple land-use and traffic predictor variables, and assimilation of data collected by mobile measurements over 30 days in the periods May–July 2022 and January–February 2023. Cross-validation was done against in-situ data extracted from the same collection, while validation was organized by comparison with standard measurements at fixed reference sites. Our study shows that this combined method has a good performance for all pollutants ($R^2 > 0.65$), the highest performance being observed for the cold season. PM_{10} concentration maps indicate multiple sources of particles during the warm season, the most important source being traffic. During the cold season PM_{10} concentration maps show a more uniform distribution of sources in Bucharest. The city's principal roads, particularly the Bucharest ring road, are also highlighted in the NO_2 maps, with higher gradient during the warm period.

1 Introduction

The atmosphere is an essential element for the environment and life forms on Earth. Therefore, any change in natural composition of the atmosphere due to the presence of one or more pollutants in the atmosphere, such as gases or aerosols released directly into the atmosphere from natural or anthropogenic sources, can dramatically influence the Earth's climate and bio-

https://doi.org/10.5194/egusphere-2024-2930
Preprint. Discussion started: 20 November 2024

sphere, human life and health, and economic activities (Nemuc et al., 2013; Kokkalis et al., 2016; Ilie et al., 2023). One major concern nowadays is the air quality in urban areas due to its significant health risks determined by prolonged population exposure to gaseous pollutants like nitrogen dioxide (NO_2), as well as to particulate matter ($PM_{2.5}$ and PM_{10}). These compounds are often associated with the onset of multiple health issues including cardiovascular diseases, asthma or lung cancer (Brunekreef and Holgate, 2002; Bernstein et al., 2004; Almetwally et al., 2020; Schmitz et al., 2019). Despite its critical impact, air pollution information in urban areas is not always available, or not at an appropriate spatial resolution, hindering effective air quality management efforts. High-resolution air quality maps are pivotal for environmental stewardship and public awareness by filling the gaps in our understanding of urban air quality. These maps can help to identify pollution hotspots, offering new opportunities for pollution mitigation strategies and influencing both policy and individual behavior (Apte et al., 2017).

Mapping pollutant concentrations in urban areas requires fine-scale spatial interpolation of data collected at air quality monitoring stations, taking into account known emission sources and sinks to estimate the actual distribution of pollutants at ambient surface level. Moreover, changes in the composition of the atmosphere caused by urban agglomeration is highly variable in space and time, making its spatial variation difficult to assess with air quality monitoring instruments from ground-based networks or on-board of satellites (Hoek et al., 2015). Fixed monitoring stations are suitable for recording temporal variation of air pollution, including long-term trends, but not proper to capture the spatial variation of air pollution at local level (Li et al., 2019).

It has been demonstrated that gradients at urban scale can be identified by mobile monitoring. High resolution mapping of air quality can be done based on long-term average of a significant number of repeated measurements. However, mobile monitoring to obtain reliable small-scale variations (for a street segment or a residential area) that are subsequently time-averaged to provide long-term concentrations is time-consuming, involving extended resources, due to the necessity to collect a large number of co-located data and in the same time to cover the whole relevant area. Several models have been developed to overcome the weakness of limited availability of the observational data, either collected at fixed locations, or during mobile campaigns, or measured by instruments onboard of satellites. Data from ground-based mobile and fixed stations as well as satellites data have been used in Land-Use Regression (LUR) models (e.g. Apte et al. (2017); Anand and Monks (2017); Messier et al. (2018); Shairsingh et al. (2019); Kerckhoffs et al. (2021, 2022a)) and dispersion models (e.g. Hamer et al. (2020); Ramacher et al. (2021); Snoun et al. (2023)). Both models have emerged as very promising and efficient tools for fine-scale mapping of the changes in the composition of the atmosphere, as well as for quantifying the air quality by long-term averaging at a high spatial resolution.

The LUR model is more widely used in air quality studies compared to dispersion modeling because: (a) it is a multivariate linear regression model built on significant covariates that can be further used to estimate pollutant concentration elsewhere, (b) linear regression is one of the most used fine-scale spatial interpolation methods because it is fast, easy to implement and does not require high computing power and, (c) a LUR model does not require detailed information on atmospheric conditions as input data (Kerckhoffs et al., 2021, 2022b). Initially, LUR models were developed to estimate the concentration of air pollutants linked with traffic emissions, specifically NO_2 and NO_x (Briggs et al., 1997; Stedman et al., 1997; Hoek et al., 2008; Eeftens et al., 2012; Lu et al., 2020; Zhang et al., 2021). Lately, LUR models have been successfully expanded to include

https://doi.org/10.5194/egusphere-2024-2930
Preprint. Discussion started: 20 November 2024

other air pollutants, such as particulate matter (PMs) (Taheri Shahraiyni and Sodoudi, 2016; Karimi and Shokrinezhad, 2021; Zhao et al., 2021; Wallek et al., 2022), ozone (O_3) (De Marco et al., 2022; Wei et al., 2022), carbon monoxide (CO) (Bi et al., 2022), and sulfur dioxide (SO_2) (Wu et al., 2019; Mikeš et al., 2023). LUR models can now estimate a wide range of air pollutants, including black carbon (BC) (Xu et al., 2021; Van den Bossche et al., 2015), volatile organic compounds (VOCs) (Zapata-Marin et al., 2022; Choi et al., 2022), and ultrafine particles (UFP) (Ge et al., 2022; Kerckhoffs et al., 2021; Lloyd et al., 2023; van Nunen et al., 2020; Jones et al., 2020; Saha et al., 2019). LUR models can be used both for specific sites, such as highways (Lee et al., 2013; Patton et al., 2014) or neighborhoods (Lim et al., 2019), as well as in detailed studies covering a wide range of land-use types across large city areas (Hatzopoulou et al., 2017; Van den Hove et al., 2020). Recent studies report on variations of pollutant levels across different times of the year, based on seasonal measurement campaigns (Xu et al., 2021; Miri et al., 2019; Shi et al., 2020).

In general, LUR models tend to "smooth" concentration levels over a wide area, leading to under or overestimation of observed concentrations within each pixel. Therefore, one of the most feasible and robust approaches to map air quality at high resolution is to use the mixed-effects modeling framework that combines the advantages of measurement-only mapping and LUR modeling (Kerckhoffs et al., 2022a, b). Mixed-effects modeling is mostly used in scenarios where data is hierarchical or clustered (e.g. Fokkema et al. (2018); Seibold et al. (2019)). In air pollution research, mixed-effects models are powerful tools that can account for spatial or temporal clustering inherent in air quality data. They can accommodate factors like geographic regions or repeated measurements over time, providing a nuanced understanding of pollutant distribution. These models can be computationally complex, especially when dealing with large datasets or complicated random effects structures (Kerckhoffs et al., 2022a).

The mixed-effects model framework has been used in recent air quality studies for urban areas, like Amsterdam and Copenhagen (Kerckhoffs et al., 2022b), Oakland (US) (Kerckhoffs et al., 2024). Also, a similar mixed-effects approach has been used to estimate NO_2 concentrations over Hong Kong (Anand and Monks, 2017). Up to now, no fine mapping of air pollutants at high spatial resolution has been performed for urban areas in Romania, although many cities face serious atmospheric pollution episodes (Marin et al., 2019; Ilie et al., 2023).

In this paper we present the development and use of the mixed modeling framework for fine-scale mapping of NO_2, PM_{10}, $PM_{2.5}$ and UFP concentrations in Bucharest, the capital of Romania. Data from two mobile measurements campaigns, representative for warm and cold seasons, were combined with fine-scale land-use parameters to provide the spatio-temporal information necessary to predict seasonal surface concentrations. Results were validated against in situ measurements from Magurele Center for Atmosphere and Radiation Studies (MARS), and eight fixed observation stations operated by the National Air Quality Monitoring Network (NAQMN). A detailed description of the study area, measurements and data treatment are given in Section 2, the mixed-effects modeling framework tuning for Bucharest is given in Section 3, together with model performance evaluation and aggregated pollutants maps for warm and cold seasons in Bucharest.

https://doi.org/10.5194/egusphere-2024-2930
Preprint. Discussion started: 20 November 2024

2 Materials and methods

2.1 Study area

Bucharest is the most populated urban area, and the most important industrial and commercial center of Romania. According to the latest census, the population of Bucharest is approximately 2.1 million residents (INS, 2024), making it the sixth-largest city in the European Union by population. The city covers an area of about 240 square kilometers and has a dense urban structure. The land use of Bucharest is diverse, the central and northern parts of the city are predominantly residential areas, characterized by a mix of old and new housing developments. The southern and western parts of Bucharest are more industrialized, hosting a variety of manufacturing plants, such as machinery, textiles, chemicals, electronics, and business parks that contribute significantly to its economic base (Ilie et al., 2023; Balaceanu et al., 2018). The surroundings of Bucharest are mostly agricultural areas and rural/pre-urban residential areas.

Located in the southeastern part of Romania, in the Romanian Plain, Bucharest belongs to the mid-latitude climate zone with a humid continental climate with four seasons, characterized by hot summers and cold winters. Due to atmospheric circulation patterns specific to the north mid-latitude zone, episodes of long-range transport of aerosols from desert regions (Sahara, Arabian Peninsula and Persia) and from wildfires can affect Bucharest's air quality. However, the major pollution sources are local, influenced by the topography, the different local-scale wind regimes and anthropocentric activities (Fenger, 1999; Grønskei, 1998; Marmureanu et al., 2017; Balaceanu et al., 2018; Marin et al., 2019; Ilie et al., 2023).

2.2 Observational data

Data was collected during two intensive mobile measurement campaigns carried out in Bucharest during May - July 2022 and January - February 2023. For each campaign, at least 15 measurement routes of approximately 100 km long and around 8 hours were carried out, under various meteorological conditions. Measurements were performed from Monday to Friday, from early morning to the afternoon, being therefore representative for daytime working times. The route comprised high-traffic streets, residential, industrial, and commercial districts, as well as suburban neighborhoods. Portable equipment measuring UFP, particle matter fractions (PM_1, $PM_{2.5}$, PM_{10}), and NO_2 were employed in both campaigns, with a measurements rate of one second. An additional GPS system has been used to independently save the precise location. A Nafion dryer was also used during warm period to reach a humidity below 40% for UFP measurements.

The mobile data has been filtered before being ingested into the model. A pass-band filter based on the moving average model with a window on 3 data points was used to remove data-points with values higher and lower than 1.5 times the window mean.

2.3 Fine-mapping model

We used the land-use regression and mixed-effects modeling framework to develop high-resolution air quality maps for Bucharest. In a LUR model, the concentration of a pollutant is expressed as a linear combination of variables that approx-

https://doi.org/10.5194/egusphere-2024-2930
Preprint. Discussion started: 20 November 2024

imates the influence of different emission sources and sinks. Usually LUR models are fixed-effect models because: (a) they use predictor variables that are temporally invariant (e.g. classes from the land cover inventories, statistical values of population density or traffic intensity, street networks) and, (b) they are applied to the average atmospheric state over the entire observation period. Therefore, LUR models based on fixed variables are not sensitive to unobserved heterogeneity arising from temporal variability in emissions or/and other environmental conditions.

The mixed-effects LUR model considered in this work is similar to the one developed in Kerckhoffs et al. (2022a). The daily mean concentration at a reference point i on day j (Y_{ij}) is assumed to be a linear function of the random effect (A_{ij}) and the predictor variables (X_{ijk}) computed at the same reference point:

$$Y_{ij} = \alpha_0 + \alpha_1 \cdot A_{ij} + \sum_{k \geqslant 0} \beta_k \cdot X_{ijk} + \in_{ij} \quad (1)$$

In Eq. (1), α_0 is the random intercept, while α_1 is the random slopes of A_{ij}, respectively. The β_k are the regression coefficients of predictor variables X_{ijk} at reference point i and day j. The regression coefficients are the same for all measurements days. The error term of the model is represented by $\in_{ij}$. Mixed model results were averaged per point, similar to the average of the data-only approach. Mean NO_2, PM_{10}, $PM_{2.5}$ and UFP concentrations from each reference point were used as the dependent variables Y_{ij} in Eq. (1).

The route taken during campaigns was divided into road segments with a length of approximately 250 m, equivalent to space traveled by a car with the average speed of 30 km/h in a time interval of 60 s. The reference points were considered at the midpoint of each road segment.

A temporal correction was applied on the data to synchronize the measurements. The correction factor is calculated for each point as the difference between the daily average values corresponding to the point and the whole-campaign average value corresponding to the same point. Values measured within a 250 m street segments were averaged for each day. Similar correction and averaging methods were reported in previous studies (e.g (Kerckhoffs et al., 2021, 2022a)).

The performance of the model has been evaluated in three steps. First, a subset of data collected through mobile measurements (and not used to tune the model) was used for cross-validation. Second, an independent set of data collected at fixed sites was used for validation. In addition to the MARS site, eight monitoring stations operated by NAQMN in Bucharest were selected for validation, based on data availability, representing all types of environments: two urban-type stations located in the east and northeast of the city, one suburban station located 4 km to the south of the capital city, three industrial-type stations situated in the southern half of the city, and two traffic-type stations located in the center of the Bucharest. The evaluation involved direct comparison of statistical metrics (correlation, root mean square error, relative differences) between model outputs and pollutant direct measurements. The last step was the evaluation of the model performance to resolve different types of environment (traffic, urban, industrial). Details and results are provided in Section 3.2.

https://doi.org/10.5194/egusphere-2024-2930
Preprint. Discussion started: 20 November 2024

3 Results and discussions

3.1 Tuning the mixed-effects Land-Use Regression model for Bucharest

Based on the specificity of the climate in the region of Bucharest, we decided to use the residential areas (predictor variable) as time-dependent variables with major differences between the warm season and the cold season (Ilie et al., 2023). Residential areas are considered sources of pollution due to household activities, heating being responsible for the major difference between the cold and the warm seasons. However, the time dependence of this variable is not sufficient to describe the day-to-day variability because the residential heating is generally switched on in late autumn and off in late spring, with no real daily variability. To model NO_2, PM_{10}, $PM_{2.5}$ and UFP concentrations over the Bucharest area, an additional variable was needed in the LUR models to cover the fast time-dependencies (the so-called "random" effects). In this mixed-effects framework, the pollutant concentration can be expressed as a linear relationship between fixed variables and time-dependent variables, where the random effect is modeled by including a discrete “dummy” variable.

In our work, for each reference point, the “random effect” was modeled as the difference between the standard deviation calculated for the entire period of mobile measurements and the standard deviation calculated for each day of mobile measurements. Therefore, the magnitude and/or sign of the “random” effect were not the same over all reference points of measurements. The mixed-effects models were fitted to the observational dataset using the Python modules scipy, sklearn and statsmodels.

Other predictor variables used for the LUR models include vehicle traffic intensity (calculated separately for the warm and for the cold seasons) as well as aggregated values of the spatial predictor variables calculated in circular buffers with radii between 25 m and 2 km.

The mixed-effects LUR models (one model for each pollutant considered in this study) were adjusted and trained for Bucharest to obtain consistent datasets. For the training process, 85% subsets of mobile measurements were randomly selected. The remaining 15% of the mobile measurements were used to cross-validate the LUR models. The regression coefficients obtained as an output of the training were further used to generate high-resolution maps of seasonal concentrations of NO_2, PM_{10}, $PM_{2.5}$ and UFP with a resolution of 100 m, over an area of approximately 240 km^2 (the entire area of the city of Bucharest).

3.1.1 Spatial predictor variables

To define the optimal configurations of LUR architectures for Bucharest, for each 250 m street segment, spatial predictor variables were extracted using the following data sources: (i) CORINE for land cover (European Environment Agency, 2018), (ii) Open Street Maps (OSM) (OpenStreetMap, 2021) for road network and (iii) National Institute of Statistics (INS) for population density.

There is no recent source quantifying the traffic intensity on road segments in Bucharest, therefore the value for this predictor was estimated for each direction of the street segment i using the following relationship:

https://doi.org/10.5194/egusphere-2024-2930
Preprint. Discussion started: 20 November 2024

$$Counts_i = \frac{N}{L} \cdot fc_i \cdot v_i \quad (2)$$

where N represents the total number of vehicles per day obtained from INS, L represents the total length of street segments (km), v_i represents the speed on the street segment (km/h), fc_i represents cost function for the street segment (h) retrieved from geofabrik.de database (Geofabrik, 2024).

In order to tune and train the mixed-effects models for the specifics of Bucharest, the spatial predictor variables were selected from a number of proxies that describe the possible sources and sinks of NO_2, PM_{10}, $PM_{2.5}$, PM_1 and UFP emissions. These variables are presented in Table 1. The column "direction of effect" represents the effect that the predictor variables have on the concentration of the pollutant in the atmosphere. Variables associated with emission sources have a positive effect, while variables associated with sinks, such as vegetation cover, have a negative effect. The circle radii most commonly used for buffering the variables describing the sources and sinks at a given location are given in column "Buffer sizes".

3.1.2 Predictor variable selection

For the selection of variables we first removed proxies with a percentage of null values greater than 90%. After applying this filter, proxies that describe the possible sources and sinks for LUR models tuned for Bucharest were associated with:

- traffic, with predictors "Counts" (number of vehicles per day) and road length variables in buffer of 50 to 1000 m
- land-use, with predictors: industry, green, residential lower density (individual residential), residential higher density (collective residential), construction and water in buffers of 100 to 2000 m
- population density in buffers of 100 to 2000 m

To determine the optimal combination of predictor variables, the supervised forward stepwise regression approach proposed within the European Study of Cohorts for Air Pollution Effects (ESCAPE) project (ESCAPE, 2024) was used. ESCAPE model starts from a constant value and after that the predictor variables are added based on the goodness of fit given by the adjusted cross-correlation (R^2) value. The direction of effect for all variables was kept as in Table 1. The variable with the highest adjusted R^2 was included in Eq. (1) as X_k. The process of building the model stops when the new variables do not contribute significantly (more than 1%) to the improvement of the adjusted R^2 value. The LUR model configurations were generated using all possible combinations of generated predictor values. From the total of the models obtained, only the LUR models for which the adjusted R^2 value was higher than 0.5 were selected.

In a second step we calculated the confidence level (p-value) and variance inflation factor (VIF) to identify that predictor's contribution to a collinearity problem. The statistically insignificant variables ($p > 0.05$) and predictor variables where VIF > 5 sequentially were not used in the model.

The predictor variables and the size of the buffers used in this work are shown in Table 1. The predictors passing the above conditions are shown in bold.

https://doi.org/10.5194/egusphere-2024-2930
Preprint. Discussion started: 20 November 2024

Table 1: Description of spatial predictor variables

Source data	**Variable name**	**Description**	**Unit**	**Effect**	**Buffer sizes (m)**
INS	**POPDENS_X**	Population density	#/m^2	+	100, 150, 200, 250, 300, 500, **1000**, 2000
CORINE 2018	**LDRES_X**	Low-density residential	m^2	+	100, 150, 200, **250**, 300, 500, 1000, 2000
	HDRES_X	High-density residential	m^2	+	100, 150, 200, 250, **300**, 500, 1000, 2000
	AIRPORT_X	Airport area	m^2	+	100, 150, 200, 250, 300, 500, 1000, 2000
	INDUSTRY_X	Industrial areas	m^2	+	100, 150, 200, **250**, 300, 500, 1000, 2000
	AGRI_X	Agricultural areas	m^2	+/-	100, 150, 200, 250, 300, 500, 1000, 2000
	FOREST_X	Forest areas	m^2	-	100, 150, 200, 250, 300, 500, 1000, **2000**
	GREEN_X	Urban green areas	m^2	-	100, 150, 200, 250, 300, 500, 1000, 2000
	CONSTR_X	Construction sites	m^2	+	100, 150, 200, **250**, 300, 500, 1000, 2000
	WATER_X	Water bodies	m^2	+/-	100, 150, 200, **250**, 300, 500, 1000, 2000

https://doi.org/10.5194/egusphere-2024-2930
Preprint. Discussion started: 20 November 2024

Road network	**LENGTH_X**	Length of road segments	m	+	25, 50, **75**, 100, 150, 200, 250, 300, 500, 1000, 2000
	TRAFFIC_X	Total traffic load	(veh / day) * m	+	25, 50, 75, 100, 150, 200, 250, 300, 500, 1000
	COUNTS	Traffic intensity	veh / day	+	NA

3.2 Evaluation of the model performances

For each individual pollutant, four configurations of LUR models were defined, out of those showing the adjusted R^2 greater than 0.5. Further, only the results and performances of the LUR models for which the highest adjusted R^2 value was obtained are discussed.

The mixed-effects model tuned for Bucharest city has been evaluated using mobile measurements and fixed-site measurements. The performance assessment involved not only the averages in some points, but also the overall agreement on specific types of urban areas covering the entire pollutants concentration intervals. The performance of each model (one for each type of pollutant) was tested in three steps. First, the outputs of the model have been cross-validated against mobile measurements on the route (the 15% randomly selected mobile datasets not used for training). Second, the average concentrations calculated by the model at the location of the fixed observation sites have been validated by comparison with the seasonal-average concentrations measured at those sites. Also, model data clustered based on the type of the environment (traffic, industrial, urban) has been compared to similarly clustered data collected at the fixed observation sites.

3.2.1 Cross-validation against mobile measurements

Cross-validation is performed for each model by comparing the model predicted dataset against the observed data collected by mobile measurements. Agreement between the two datasets is quantified by calculating the adjusted R^2 and root mean square error (RMSE). The RMSE of each model was calculated as the square root of the mean of the squared errors. We also present the relative differences between modeled and measured data as a general indicator of the model accuracy. Results show very good correlations ($R^2 > 0.91$) for each model as a follow-up of the training process. The cross-validation shows higher correlations for the cold season (R^2 = 0.81 for NO_2 and R^2 = 0.88 for PM_{10}) than for the warm season (R^2 = 0.59 for NO_2 and R^2 = 0.72 for PM_{10}). The weaker performance of the models during the warm season can be explained by the large variability of NO_2 and PM_{10} concentrations in the warm season compared to the cold season (Ilie et al., 2023), which is not completely captured by our method. Moreover, this strong variability is also suggested by the RMSE values which for the NO_2 are higher in the warm season (8.62 ppb) than in the cold season (6.99 ppb). In contrast, the RMSE values for PM_{10} are lower in the warm season (4.74 μg/m^3) than in the cold season (9.38 μg/m^3).

https://doi.org/10.5194/egusphere-2024-2930
Preprint. Discussion started: 20 November 2024

The relative differences between mobile measurements and model retrievals, computed as (Model-Observed)/Observed, show the ability of the models to estimate PM_{10} and NO_2 concentrations (Fig. 1). It can be seen that the model for NO_2 tends to overestimate the predicted concentrations in the warm season, especially in urban agglomeration areas (upper left panel), while the model for PM_{10} tends to underestimate the predicted concentrations(lower left panel). However, such differences are acceptable considering the assumptions made, the uncertainty of the data used for training the models, as well as the general performances reported in the literature (Ma et al., 2024).

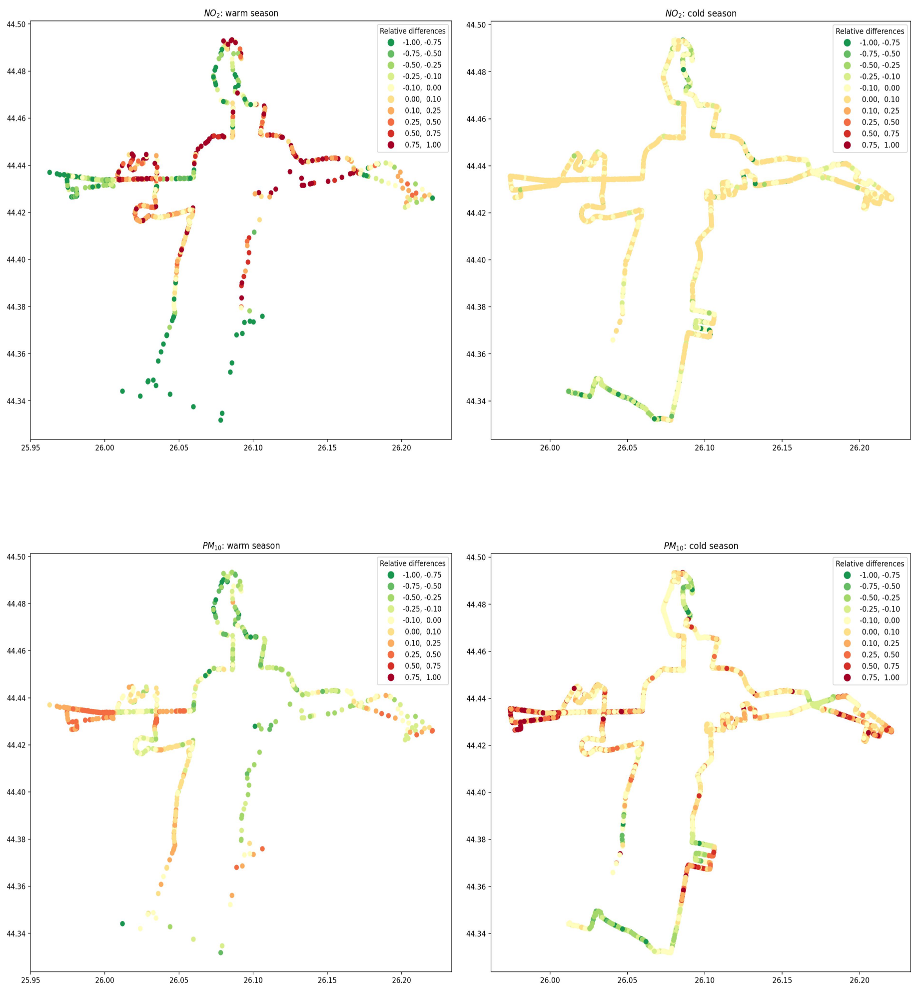

Figure 1. Relative difference between model predicted values and mobile measurements of NO_2 (upper panel) and PM_{10} (lower panel) during warm (left panel) and cold (right panel) season

https://doi.org/10.5194/egusphere-2024-2930
Preprint. Discussion started: 20 November 2024

3.2.2 Validation against independent measurements at fixed observation sites

The model output was evaluated against the seasonal average of the hourly values of NO_2 and PM_{10} measured at nine long-term operated in situ stations, out of which eight stations operated by NAQMN. These sites are considered representative for urban, industrial and suburban areas as pictured in Fig. 2. The model could not be evaluated in the case of UFP, due to unavailability of the data at all fixed stations. Statistical metrics, like R^2, RMSE and relative differences were calculated similarly as for the cross-validation. Statistical parameters are summarized in Table 2.

In Fig. 2, the mean mass concentrations measured at the fixed observation sites are represented by the diameter of the circle, and the type of the environment is represented by the color of the circle. It can be seen that the variation of the concentrations across the city is relatively low, especially for particulate matter during the cold season. PM_{10} concentrations range from 21 to 32 $\mu g/m^3$ in both seasons. The highest PM_{10} concentrations are observed at the urban, sub-urban and the traffic stations, while the lowest PM_{10} concentration is measured at the industrial stations. The western part of the city shows highest PM_{10} values. NO_2 concentrations range from 8 to 20 ppb in the warm season and from 9 to 24 ppb in the cold season. The highest NO_2 concentrations correspond to the areas with intense traffic and industrial activities, while the lowest concentrations are observed in the sub-urban areas, which are less impacted by traffic.

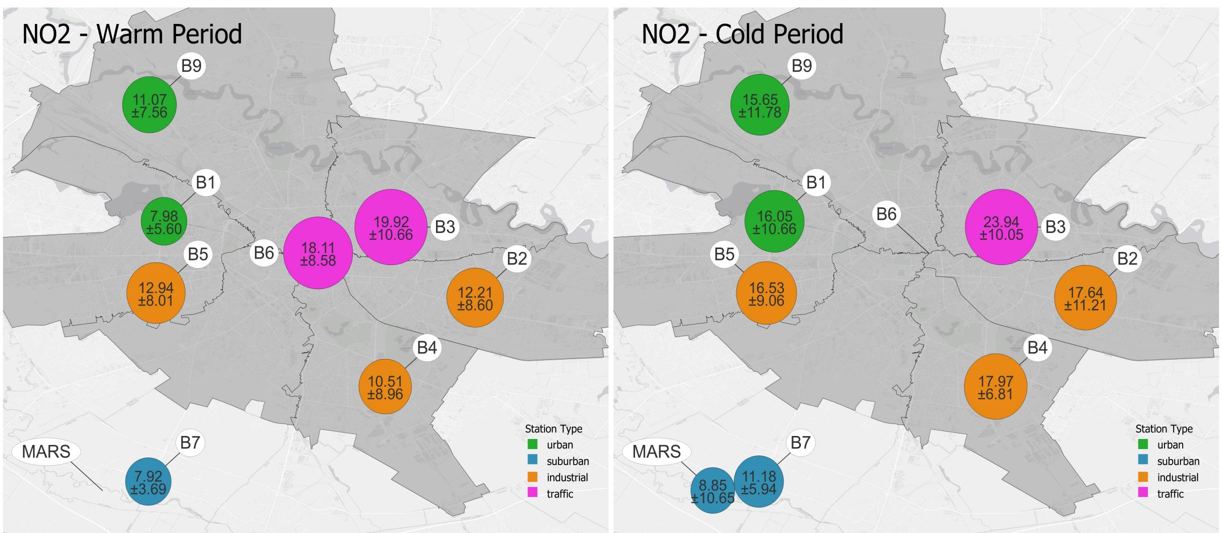

https://doi.org/10.5194/egusphere-2024-2930
Preprint. Discussion started: 20 November 2024

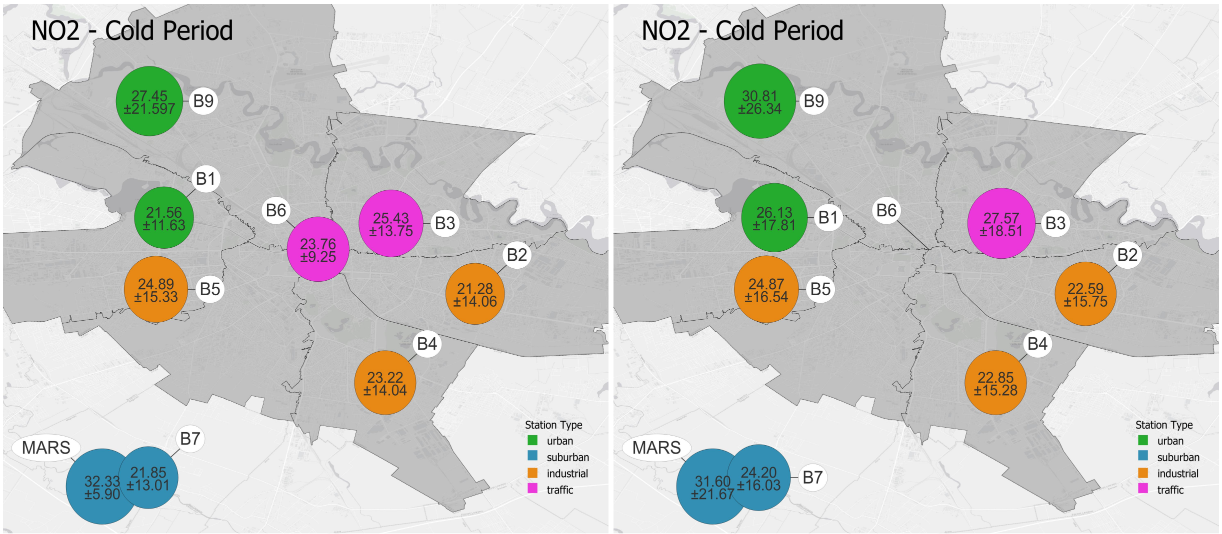

Figure 2. Average concentration of NO_2 (upper panel, units ppb) and PM_{10} (lower panel, units $\mu g/m^3$) during warm (left panel) and cold (right panel) season at fixed sites: the diameter of the circle represents the mean mass concentrations measured at the site; the color of the circle represents the type of the environment at the site

.

The comparison between model predicted values and the observed values at the nine fixed sites is presented in Table 2. Overall, the model performed well, even if the NO_2 values tend to be slightly overestimated, and PM_{10} tend to be slightly underestimated when compared with measured mean concentrations. Mean values of modeled NO_2 are within the range of the observed values, as indicated by the standard deviation. The differences can be explained by the local topography and the specifics of the land use. The road system in Bucharest is very dense, so the distance from a street to residential or industrial sectors is often very short, sometimes less than few meters, therefore the NO_2 100 x 100 m grid resolution cannot always resolve the variations. This "smoothing" effect caused by insufficient spatial resolution of the model is pin pointed by the lower values of the standard deviations returned by the model by comparison with those returned by observations.

The trends and seasonal differences of both NO_2 and PM_{10} are well resolved by the model, as shown by the comparison with observations. The R^2 correlation between observed mean concentrations and modeled mean concentration is above 0.65 for all pollutants for warm season, and 0.75 for cold season. These values can be attributed to the good performance of the model, in accordance with the values reported for other cities (Yuan et al., 2023). The lowest correlation value is noted for particulate matter during warm season. This result can be explained by the fact that, during the warm season, photo-chemical processes are intensified at the street level, and the model cannot capture the effects properly.

The RMSE is another important parameter for assessing the performance of the model, accounting for the level of absolute error. As in the case of R^2, we noticed a better model performance for the cold season. The difficulties of the model to capture

https://doi.org/10.5194/egusphere-2024-2930
Preprint. Discussion started: 20 November 2024

the small variations during the warm period for both NO_2 and PM_{10} are depicted by higher RMSE values. High values of RMSE correspond to low R^2 values, demonstrating that the model cannot fully capture the variations of NO_2 or PM_{10} concentrations.

Table 2. Comparison between model output and measured values at fixed sites for NO_2 and PM_{10} in Bucharest (Romania) during warm period 2022 and cold period 2023, and statistical metrics

Pollutant	Season	Observed mean concentration	Modelled mean concentration	R^2	RMSE
NO_2	warm	12.58 ± 7.71 ppb	16.38 ± 2.47 ppb	0.66	4.97 ppb
	cold	15.98 ± 9.52 ppb	17.25 ± 1.17 ppb	0.75	2.27 ppb
PM_{10}	warm	$24.64 \pm 13.18\ \mu g/m^3$	$24.29 \pm 4.38\ \mu g/m^3$	0.65	$2.02\ \mu g/m^3$
	cold	$26.33 \pm 18.50\ \mu g/m^3$	$25.64 \pm 4.43\ \mu g/m^3$	0.76	$1.69\ \mu g/m^3$

3.2.3 Evaluation of the model performance to resolve different types of environment

The model was tested for its robustness in capturing differences between various types of environment such as urban (including pre-urban), industrial, traffic. Long-term datasets collected at the nine fixed observation sites were used for this purpose. Figure 3 shows mean concentrations of NO_2 and PM_{10} as retrieved by the model and measured at the stations, clustered by the type of environment and separated for the warm and cold seasons. The relative differences between values modeled and measured in different environments are also highlighted.

NO_2 is the most variable species, with high differences between seasons and between environment types. Lower NO_2 concentrations are depicted for the urban group, whereas the highest NO_2 concentration is associated to traffic, as anticipated. The traffic group has the lowest variability among seasons and is also better captured by the model. The model shows increased NO_2 concentrations during the warm season for urban and industrial categories, while in the case of traffic areas the model underestimate a bit the measurements averages. The overall relative differences between cold and warm seasons for both model and observational data inside each defined environment is less than 35%. Higher relative differences between modeled and measured data are observed for warm season for all areas, with lowest difference in the case of traffic areas, around 10%. Overall lower relative differences between modeled and measured data are observed during cold season in comparison with warm period, with NO_2 average concentration in industrial and traffic areas underestimated by the model, highlighted by relative differences up to -20%.

PM_{10} concentrations show an overall lower seasonal variability, and also lower differences between model and observed data, with relative differences less than 20%. Particulate matter concentrations for urban, industrial, and traffic areas varied slightly among seasons. Modeled PM_{10} concentrations shows higher values for industrial environment in comparison with observational data for both seasons. Moreover, industrial areas present the lowest PM_{10} concentration during cold season, as shown by both modeled and measured data. Urban and traffic environment PM_{10} concentrations are slightly underestimated

https://doi.org/10.5194/egusphere-2024-2930
Preprint. Discussion started: 20 November 2024

by the model. The overall relative differences of PM_{10} concentration between cold and warm seasons for both model and observational data inside each defined environment is less than 15%. Small relative differences between modeled and measured data are observed for PM_{10} concentrations, during both seasons. PM_{10} average concentration in urban and traffic areas are slightly underestimated by the model, highlighted by relative differences up to -10%.

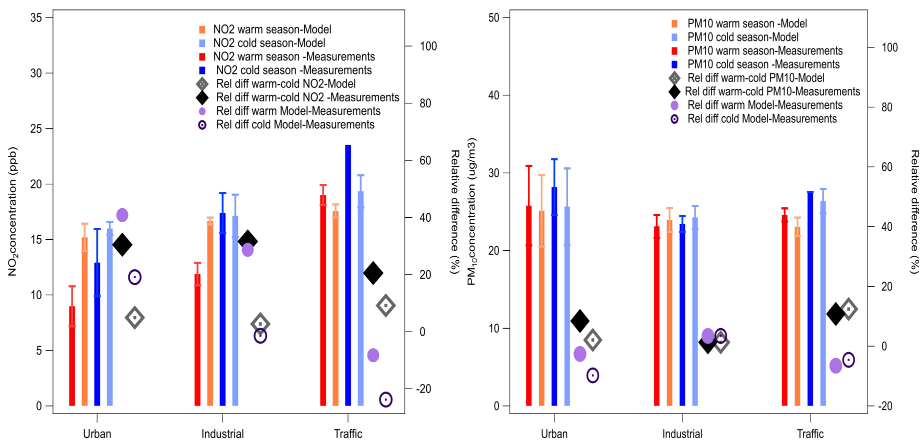

Figure 3. Model (light color) versus measurements (dark color) mean concentrations of NO_2 (left panel) and PM_{10} (right panel) during warm (red) and cold (blue) seasons, along with the relative difference between cold and warm season from model (grey diamond mark) or measurements (black diamond mark); relative difference between model and measurements for warm (purple circle mark) and cold (dark purple circle mark) seasons

3.3 Mapping atmospheric pollution in Bucharest

The validated model was further used to produce NO_2, PM_{10} and UFP concentrations maps for Bucharest, representative for the warm and cold seasons (Fig. 4). The results are valid for daytime and working days of the week. In analyzing these results, it must be noted that the near-surface concentrations of atmospheric pollutants are influenced not only by the emissions, but also by the height of the planetary boundary layer, transport from other regions, dry and wet deposition and chemical processes, all in relation to relatively fast changing meteorological conditions (e.g. air temperature, wind field). Model results show that, overall and regardless the season, NO_2, PM_{10} and UFP concentrations are higher on the main road sections, with higher values on Bucharest's western area.

NO_2 concentration maps show that this pollutant is highly related to traffic, the road network of Bucharest being clearly visible both during the warm and during the cold season. The main roadways, especially the Bucharest ring road, are depicted as the primary NO_2 source. Also, featured are the city central routes, where traffic remains heavy throughout the day and seasons. The highest NO_2 concentrations is noted around busy highways due to the presence of a large number of NO-emitting automobiles. Sinks related to the green areas and water bodies regions are identified in green colors. Overall, NO_2 concentration is higher during the warm period, when concentrations are higher on key roadways (35.79 ± 8.38 ppb) and other sources in

https://doi.org/10.5194/egusphere-2024-2930
Preprint. Discussion started: 20 November 2024

the city add up. The conversion of NO to NO_2 in the presence of sunlight and ozone is significant. During cold months, the NO_2 concentration is lower in absolute values across the city, however the main roads are still depicted as major sources, followed by several industrial areas such as power plants serving the centralized heating of the city. The distribution of the NO_2 concentration on all street segments is almost uniform during cold season, with a slight increase on the main street segments, including the Bucharest ring road (20.67 $\pm$ 3.44 ppb). At the level of the city of Bucharest, the average value of the NO_2 concentration as estimated by the model for the warm season is 16.66 $\pm$ 4.04 ppb, while for the cold season it is 18.75 $\pm$ 1.98 ppb.

The spatial variation of PMs in the city area is substantial, with an abundance of small particles and a high mass concentration of larger particles in densely populated residential areas. Significant concentrations of particles have been identified, mostly in industrial areas and anthropocentric agglomerations, but also along certain major transportation routes. During the cold periods, the PMs (all sizes) have larger loading and lower gradients, as reported also for other cities (Ndiaye et al., 2024). This is related to increased emissions from residential heating. A gradient of PM_{10} concentrations is evidenced within the city, with higher loading in the western and southern areas. Average PM_{10} concentration in Bucharest during cold season is 1.2 times higher than in the warm season. During the warm periods, the PM_{10} clusters are localized around source areas, while during cold periods, the sources are more homogeneous.

The average UFP number concentration throughout the mobile route exhibits an important spatial gradient, particularly during the warm season, with variations up to a factor of two in the mean, highlighting extensive human exposure to ultrafine particles. The UFP number concentrations are elevated on the main roads, as well as on some areas related to industrial activities in southern, northern and western city regions, mostly during the warm season. A more uniform distribution of UFP mean number concentration is observed during the cold season, when the house heating emissions add up to the traffic. Traffic sources are less effective during the cold season, when the chemical processes are reduced under reduced sunlight. House heating sources, more evenly distributed at spatial scale than the roads, generate more homogeneous distribution but also larger absolute values of UFP. Average seasonal concentration on Bucharest city during the cold season (29132 $\pm$ 4362 particles/cm^3) is 1.4 times higher than in the case of warm season (21469 $\pm$ 3528 particles/cm^3).

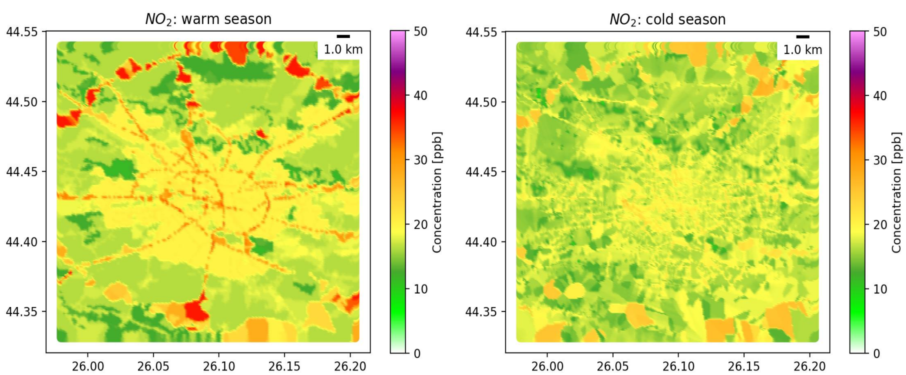

https://doi.org/10.5194/egusphere-2024-2930
Preprint. Discussion started: 20 November 2024

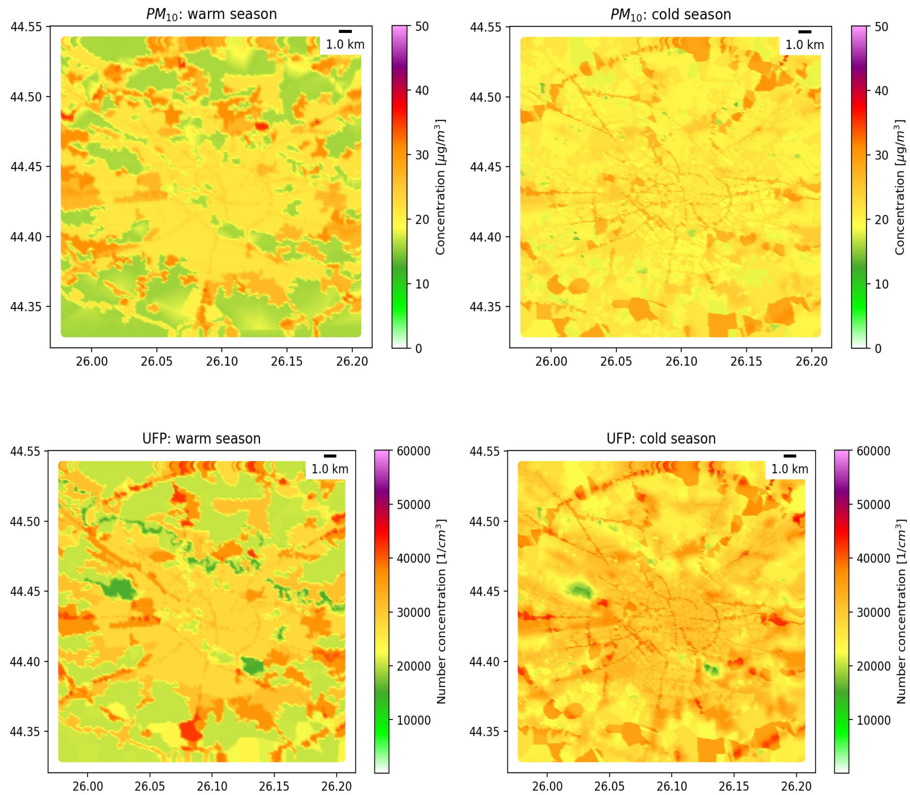

Figure 4. Near-surface concentration maps for Bucharest, as resulted from the model for NO_2, PM_{10} and UFP during warm (left panel) and cold (right panel) seasons

The fine particle fraction ($PM_{2.5}/PM_{10}$) is larger during cold than during warm periods, as expected, with fine particles accounting for up to 90% of the PM_{10} concentration. This is explained by the fact that house heating generates predominantly small particles. By comparison, during warm periods fine particle fraction is approximately 70%, still showing a significant share (Fig. 5). The main rivers and lakes within Bucharest's perimeter are clearly sinks for small particles, producing lower fine mode fractions.

https://doi.org/10.5194/egusphere-2024-2930
Preprint. Discussion started: 20 November 2024

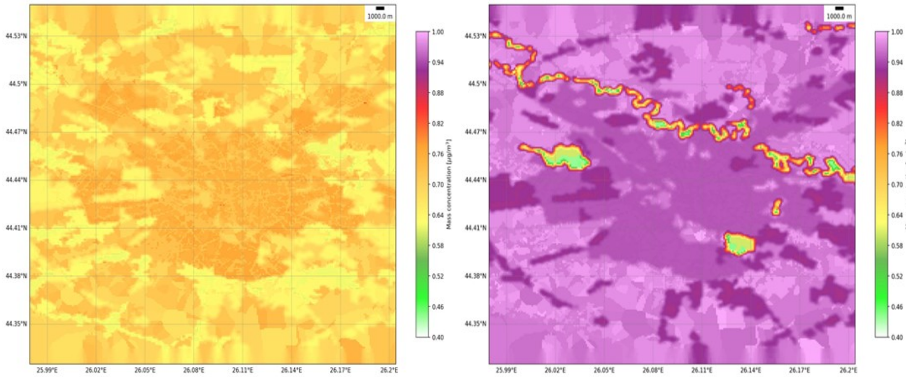

Figure 5. Model maps of $PM_{2.5}/PM_{10}$ ratio during warm and cold seasons

4 Conclusions

The regression-based methods fed by mobile data can predict NO_2, PM_{10} and UFP concentrations for regions which are not properly covered by observations. In order to do this, the right combination of data sampling frequency, duration and route, and the correct number and type of predictor factors (corresponding to the surrounding environment) must be considered. Mobile monitoring together with modeling tools can therefore compensate for spatial and temporal data gaps which are collected by the monitoring stations, and can assist individuals and policymakers in identifying regions and causes of poor air quality. In this study we demonstrate the effectiveness of combining mobile measurements with mixed-effects LUR models to derive seasonal maps of near-surface PM_{10}, NO_2 and UFP. The study shows first-time validated results for Bucharest, the capital city of Romania, which is characterized by a large, densely populated surface with a very dense and heavily used street network.

Despite the limited number of fixed stations available for this work (8 + MARS), the tuned mixed-effects LUR model proved to be robust and accurate in producing high-resolution mapping of NO_2, PM_{10} and UFP for the warm and the cold seasons. Overall, good model performance was observed for both seasons and all concentrations, similar to other studies. The slightly higher mean squared error values correlated with smaller cross-validation R^2 values obtained for the warm season suggest that the mobile campaign data collected for this study did not capture all the important NO_2 and PM_{10} concentration variations. Even if the route selected for the two mobile measurement campaigns included all urban structures, the limitation of car access remains a source of error, which can lead to underestimation the concentration of pollutants. The performance of this model can be greatly improved by the involvement of citizens (pedestrian or by bicycle) to collect data from areas where cars are not allowed. Further improvements could also be made by the inclusion of spatio-temporal emission data with a high spatial resolution, such as traffic volumes or emission inventories.

The results provided by the model show that high concentrations of particulate matter during the cold season are representative for Bucharest city, due to the added effect of house heating (either dispersed in residential areas, or localized at the city's power plants). Fine particles dominate during the cold season, although remaining at high levels during the warm season also. NO_2 is less challenging but still an important factor, especially during the warm season and along the main roads. The sea-

https://doi.org/10.5194/egusphere-2024-2930
Preprint. Discussion started: 20 November 2024

sonal high-resolution air quality maps for Bucharest based on mixed-effects modeling pin pointed pollutant variability mostly during warm season and higher concentrations and fine particles ratio during the cold season. Water and vegetation areas are evidenced as effective sinks for NO_2 and fine particles, while traffic and residential heating are evidenced as effective sources in Bucharest.

The approach presented in this paper can be adjusted for resolving high resolution mapping of NO_2, PMs and UFP in other cities as well, as long as the urban structures are well-characterized and there is as a fairly dense and diverse network of in situ monitoring stations of which observational data can be used for model calibration and validation.

Code availability. Codes developed for this study are available from the main author (Camelia Talinau, camelia@inoe.ro) upon request.

Data availability. Data used in this study are available from the main author (Camelia Talinau, camelia@inoe.ro) upon request.

Author contributions. **Camelia Talianu**: Conceptualization, Methodology, Formal analysis, Software, Writing – original draft, Writing – review & editing. **Jeni Vasilescu**: Conceptualization, Formal Analysis, Methodology, Resources, Supervision, Writing – original draft, Writing – review & editing. **Doina Nicolae**: Conceptualization, Funding acquisition, Project administration, Resources, Supervision, Writing – original draft, Writing – review & editing. **Alexandru Ilie**: Data curation; Investigation; Visualization; Writing – original draft. **Andrei Dandocsi**: Formal analysis, Investigation; Writing – original draft. **Anca Nemuc**: Writing – review & editing. **Livio Belegante**: Data curation; Investigation; Formal analysis.

Competing interests. The authors declare that they have no competing interests

Acknowledgements. We thank INCAS and INOESY for making available the mobile instruments. Also, we thank BOKU-Met, Vienna, Austria for facilitating access to the supercomputer from the IT infrastructure used for the LUR models. This publication has been prepared using European Union's Copernicus Land Monitoring Service. We gratefully acknowledge the National Air Quality Monitoring Network, part of the Ministry of Environment and the Romanian Institute of Statistics for providing invaluable data essential to this research. We appreciate the anonymous reviewers and editors for their time and effort to improve the paper.

Funding

This work was carried out through RI-URBANS project (Research Infrastructures Services Reinforcing Air Quality Monitoring Capacities in European Urban & Industrial Areas, European Union's Horizon 2020 research and innovation program under

https://doi.org/10.5194/egusphere-2024-2930
Preprint. Discussion started: 20 November 2024

grant agreement, Grant Agreement number 101036245), ATMO-ACCESS project (European Commission under the Horizon 2020 – Research and Innovation Framework Programme, H2020-INFRAIA-2020-1, Grant Agreement number: 10100800) and the Core Program within the National Research Development and Innovation Plan 2022–2027, carried out with the support of MCID, project no. PN 23 05.

https://doi.org/10.5194/egusphere-2024-2930
Preprint. Discussion started: 20 November 2024

References

Almetwally, A., Bin-Jumah, M., and Allam, A.: Ambient air pollution and its influence on human health and welfare: an overview, Environmental Science and Pollution Research, 27, https://doi.org/10.1007/s11356-020-09042-2, 2020.

Anand, J. S. and Monks, P. S.: Estimating daily surface NO 2 concentrations from satellite data–a case study over Hong Kong using land use regression models, Atmospheric Chemistry and Physics, 17, 8211–8230, https://doi.org/https://doi.org/10.5194/acp-17-8211-2017, 2017.

Apte, J. S., Messier, K. P., Gani, S., Brauer, M., Kirchstetter, T. W., Lunden, M. M., Marshall, J. D., Portier, C. J., Vermeulen, R. C., and Hamburg, S. P.: High-resolution air pollution mapping with Google street view cars: exploiting big data, Environmental science & technology, 51, 6999–7008, https://doi.org/https://doi.org/10.1021/acs.est.7b00891, 2017.

Balaceanu, C., Mitiu, M., Marcus, I., and Mincu, M.: Pollution Impact of the Grozavesti Thermoelectric Power Plant on the Urban Agglomeration Bucharest, Revista de Chimie, 69, 350–353, https://doi.org/10.37358/RC.18.2.6105, 2018.

Bernstein, J. A., Alexis, N., Barnes, C., Bernstein, I. L., Nel, A., Peden, D., Diaz-Sanchez, D., Tarlo, S. M., Williams, P. B., and Bernstein, J. A.: Health effects of air pollution, Journal of Allergy and Clinical Immunology, 114, 1116–1123, https://doi.org/https://doi.org/10.1016/j.jaci.2004.08.030, 2004.

Bi, J., Zuidema, C., Clausen, D., Kirwa, K., Young, M., Gassett, A., Seto, E., Sampson, P., Larson, T., Szpiro, A., Sheppard, L., and Kaufman, J.: Within-City Variation in Ambient Carbon Monoxide Concentrations: Leveraging Low-Cost Monitors in a Spatiotemporal Modeling Framework, Environmental health perspectives, 130, 97 008, https://doi.org/10.1289/EHP10889, 2022.

Briggs, D. J., Collins, S., Elliott, P., Fischer, P., Kingham, S., Lebret, E., Pryl, K., Reeuwijk, H. V., Smallbone, K., and Veen, A. V. D.: Mapping urban air pollution using GIS: a regression-based approach, International Journal of Geographical Information Science, 11, 699–718, 1997.

Brunekreef, B. and Holgate, S.: Air Pollution and Health, Lancet, 360, 1233–42, https://doi.org/10.1016/S0140-6736(02)11274-8, 2002.

Choi, J., Henze, D. K., Cao, H., Nowlan, C. R., González Abad, G., Kwon, H.-A., Lee, H.-M., Oak, Y. J., Park, R. J., Bates, K. H., Maasakkers, J. D., Wisthaler, A., and Weinheimer, A. J.: An Inversion Framework for Optimizing Non-Methane VOC Emissions Using Remote Sensing and Airborne Observations in Northeast Asia During the KORUS-AQ Field Campaign, Journal of Geophysical Research: Atmospheres, 127, e2021JD035 844, https://doi.org/https://doi.org/10.1029/2021JD035844, 2022.

De Marco, A., Garcia-Gomez, H., Collalti, A., Khaniabadi, Y. O., Feng, Z., Proietti, C., Sicard, P., Vitale, M., Anav, A., and Paoletti, E.: Ozone modelling and mapping for risk assessment: An overview of different approaches for human and ecosystems health, Environmental Research, 211, 113 048, https://doi.org/https://doi.org/10.1016/j.envres.2022.113048, 2022.

Eeftens, M., Tsai, M.-Y., Ampe, C., Anwander, B., Beelen, R., Bellander, T., Cesaroni, G., Cirach, M., Cyrys, J., de Hoogh, K., Nazelle, A. D., de Vocht, F., Declercq, C., Dėdelė, A., Eriksen, K., Galassi, C., Gražulevičienė, R., Grivas, G., Heinrich, J., Hoffmann, B., Iakovides, M., Ineichen, A., Katsouyanni, K., Korek, M., Krämer, U., Kuhlbusch, T., Lanki, T., Madsen, C., Meliefste, K., Mölter, A., Mosler, G., Nieuwenhuijsen, M., Oldenwening, M., Pennanen, A., Probst-Hensch, N., Quass, U., Raaschou-Nielsen, O., Ranzi, A., Stephanou, E., Sugiri, D., Udvardy, O., Éva Vaskövi, Weinmayr, G., Brunekreef, B., and Hoek, G.: Spatial variation of PM2.5, PM10, PM2.5 absorbance and PMcoarse concentrations between and within 20 European study areas and the relationship with NO2 – Results of the ESCAPE project, Atmospheric Environment, 62, 303–317, 2012.

ESCAPE: ESCAPE - Enhancing Sales Capacity for Agrifood Products in Europe, http://escapeproject.eu/, accessed: 2024-07-11, 2024.

European Environment Agency: CORINE Land Cover (CLC) 2018 dataset, Data file, https://www.eea.europa.eu/publications/COR0-landcover, accessed: 2024-08-13, 2018.

Fenger, J.: Urban air quality, Atmospheric environment, 33, 4877–4900, 1999.

Fokkema, M., Smits, N., Zeileis, A., Hothorn, T., and Kelderman, H.: Detecting treatment-subgroup interactions in clustered data with generalized linear mixed-effects model trees, Behavior Research Methods, 50, 2016–2034, https://doi.org/10.3758/s13428-017-0971-x, 2018.

Ge, Y., Fu, Q., Yi, M., Chao, Y., Lei, X., Xu, X., Yang, Z., Hu, J., Kan, H., and Cai, J.: High spatial resolution land-use regression model for urban ultrafine particle exposure assessment in Shanghai, China, Science of The Total Environment, 816, 151 633, 2022.

Geofabrik: Geofabrik GmbH, https://download.geofabrik.de/, accessed: 2024-07-11, 2024.

Grønskei, K. E.: Europe and its cities, in: Urban Air Pollution—European Aspects, pp. 21–32, Springer, 1998.

Hamer, P. D., Walker, S.-E., Sousa-Santos, G., Vogt, M., Vo-Thanh, D., Lopez-Aparicio, S., Schneider, P., Ramacher, M. O., and Karl, M.: The urban dispersion model EPISODE v10. 0–Part 1: An Eulerian and sub-grid-scale air quality model and its application in Nordic winter conditions, Geoscientific Model Development, 13, 4323–4353, 2020.

Hatzopoulou, M., Valois, M.-F., Levy, I., Mihele, C., Lu, G., Bagg, S., Minet, L., and Brook, J.: Robustness of Land-Use Regression Models Developed from Mobile Air Pollutant Measurements, Environmental Science & Technology, 51, https://doi.org/10.1021/acs.est.7b00366, 2017.

Hoek, G., Beelen, R., de Hoogh, K., Vienneau, D., Gulliver, J., Fischer, P., and Briggs, D.: A review of land-use regression models to assess spatial variation of outdoor air pollution, Atmospheric Environment, 42, 7561–7578, 2008.

Hoek, G., Eeftens, M., Beelen, R., Fischer, P., Brunekreef, B., Boersma, K., and Veefkind, P.: Satellite NO2 data improve national land use regression models for ambient NO2 in a small densely populated country, Atmospheric Environment, 105, https://doi.org/10.1016/j.atmosenv.2015.01.053, 2015.

Ilie, A., Vasilescu, J., Talianu, C., Ioja, C., and Nemuc, A.: Spatiotemporal Variability of Urban Air Pollution in Bucharest City, Atmosphere, 14, 1759, https://doi.org/10.3390/atmos14121759, 2023.

INS: National Institute of Statistics of Romania, https://insse.ro/cms/en, accessed: 2024-07-11, 2024.

Jones, R. R., Hoek, G., Fisher, J. A., Hasheminassab, S., Wang, D., Ward, M. H., Sioutas, C., Vermeulen, R., and Silverman, D. T.: Land use regression models for ultrafine particles, fine particles, and black carbon in Southern California, Science of The Total Environment, 699, 134 234, https://doi.org/https://doi.org/10.1016/j.scitotenv.2019.134234, 2020.

Karimi, B. and Shokrinezhad, B.: Spatial variation of ambient PM2.5 and PM10 in the industrial city of Arak, Iran: A land-use regression, Atmospheric Pollution Research, 12, 101 235, https://doi.org/https://doi.org/10.1016/j.apr.2021.101235, 2021.

Kerckhoffs, J., Hoek, G., Gehring, U., and Vermeulen, R.: Modelling nationwide spatial variation of ultrafine particles based on mobile monitoring, Environment International, 154, 106 569, 2021.

Kerckhoffs, J., Khan, J., Hoek, G., Yuan, Z., Ellermann, T., Hertel, O., Ketzel, M., Jensen, S. S., Meliefste, K., and Vermeulen, R.: Mixed-effects modeling framework for Amsterdam and Copenhagen for outdoor NO2 concentrations using measurements sampled with google street view cars, Environmental science & technology, 56, 7174–7184, https://doi.org/10.1021/acs.est.1c05806, 2022a.

Kerckhoffs, J., Khan, J., Hoek, G., Yuan, Z., Hertel, O., Ketzel, M., Jensen, S. S., Al Hasan, F., Meliefste, K., and Vermeulen, R.: Hyperlocal variation of nitrogen dioxide, black carbon, and ultrafine particles measured with Google Street View cars in Amsterdam and Copenhagen, Environment International, 170, 107 575, https://doi.org/https://doi.org/10.1016/j.envint.2022.107575, 2022b.

Kerckhoffs, J., Hoek, G., and Vermeulen, R.: Mobile monitoring of air pollutants; performance evaluation of a mixed-model land use regression framework in relation to the number of drive days., Environmental Research, 240, 117 457, https://doi.org/https://doi.org/10.1016/j.envres.2023.117457, 2024.

https://doi.org/10.5194/egusphere-2024-2930
Preprint. Discussion started: 20 November 2024

Kokkalis, P., Amiridis, V., Allan, J., Papayannis, A., Solomos, S., Binietoglou, I., Bougiatioti, A., Tsekeri, A., Nenes, A., Rosenberg, P., Marenco, F., Marinou, E., Vasilescu, J., Nicolae, D., Coe, H., Bacak, A., and Chaikovsky, A.: Validation of LIRIC aerosol concentration retrievals using airborne measurements during a biomass burning episode over Athens, Atmospheric Research, 183, https://doi.org/10.1016/j.atmosres.2016.09.007, 2016.

Lee, K., Wu, J., Hudda, N., Fruin, S., and Delfino, R.: Modeling the Concentrations of On-Road Air Pollutants in Southern California, Environmental science & technology, 47, https://doi.org/10.1021/es401281r, 2013.

Li, H. Z., Gu, P., Ye, Q., Zimmerman, N., Robinson, E. S., Subramanian, R., Apte, J. S., Robinson, A. L., and Presto, A. A.: Spatially dense air pollutant sampling: Implications of spatial variability on the representativeness of stationary air pollutant monitors, Atmospheric Environment: X, 2, 100 012, 2019.

Lim, C., Kim, H., Vilcassim, M. J. R., Thurston, G., Gordon, T., Chen, L.-C., Lee, K., Heimbinder, M., and Kim, S.-Y.: Mapping urban air quality using mobile sampling with low-cost sensors and machine learning in Seoul, South Korea, Environment International, 131, 105 022, https://doi.org/10.1016/j.envint.2019.105022, 2019.

Lloyd, M., Ganji, A., Xu, J., Venuta, A., Simon, L., Zhang, M., Saeedi, M., Yamanouchi, S., Apte, J., Hong, K., Hatzopoulou, M., and Weichenthal, S.: Predicting spatial variations in annual average outdoor ultrafine particle concentrations in Montreal and Toronto, Canada: Integrating land use regression and deep learning models, Environment International, 178, 108 106, https://doi.org/https://doi.org/10.1016/j.envint.2023.108106, 2023.

Lu, M., Soenario, I., Helbich, M., Schmitz, O., Hoek, G., van der Molen, M., and Karssenberg, D.: Land use regression models revealing spatiotemporal co-variation in NO2, NO, and O3 in the Netherlands, Atmospheric Environment, 223, 117 238, 2020.

Ma, X., Zou, B., Deng, J., Gao, J., Longley, I., Xiao, S., Guo, B., Wu, Y., Xu, T., Xu, X., et al.: A comprehensive review of the development of land use regression approaches for modeling spatiotemporal variations of ambient air pollution: A perspective from 2011 to 2023, Environment International, p. 108430, 2024.

Marin, C., Marmureanu, L., Radu, C., Dandocsi, A., Stan, C., Toanca, F., Preda, L., and Antonescu, B.: Wintertime Variations of Gaseous Atmospheric Constituents in Bucharest Peri-Urban Area, Atmosphere, 10, 478, https://doi.org/10.3390/atmos10080478, 2019.

Marmureanu, L., Vasilescu, J., Stefanie, H., and Talianu, C.: Chemical and optical characterization of submicronic aerosol sources, Environmental Engineering and Management Journal, 16, 2165–2172, https://doi.org/10.30638/eemj.2017.223, 2017.

Messier, K. P., Chambliss, S. E., Gani, S., Alvarez, R., Brauer, M., Choi, J. J., Hamburg, S. P., Kerckhoffs, J., LaFranchi, B., Lunden, M. M., et al.: Mapping air pollution with Google Street View cars: Efficient approaches with mobile monitoring and land use regression, Environmental science & technology, 52, 12 563–12 572, https://doi.org/https://doi.org/10.1021/acs.est.8b03395, 2018.

Mikeš, O., Sanka, O., Rafajová, A., Vlaanderen, J., Chen, J., Hoek, G., Klanova, J., and Cupr, P.: Development of historic monthly land use regression models of SO2, NOx and suspended particulate matter for birth cohort ELSPAC, Atmospheric Environment, 301, 119 688, https://doi.org/10.1016/j.atmosenv.2023.119688, 2023.

Miri, M., Ghassoun, Y., Dowlatabadi, A., Ebrahimnejad, A., and Löwner, M.-O.: Estimate annual and seasonal PM1, PM2.5 and PM10 concentrations using land use regression model, Ecotoxicology and Environmental Safety, 174, https://doi.org/10.1016/j.ecoenv.2019.02.070, 2019.

Ndiaye, A., Shen, Y., Kyriakou, K., Karssenberg, D., Schmitz, O., Flückiger, B., Hoogh, K. d., and Hoek, G.: Hourly land-use regression modeling for NO2 and PM2.5 in the Netherlands, Environmental Research, 256, 119 233, https://doi.org/10.1016/j.envres.2024.119233, 2024.

Nemuc, A., Stachlewska, I., Vasilescu, J., Górska, A., Nicolae, D., and Talianu, C.: Optical Properties of Long-Range Transported Volcanic Ash over Romania and Poland During Eyjafjallajökull Eruption in 2010, Acta Geophysica, 62, 350–366, https://doi.org/10.2478/s11600-013-0180-7, 2013.

OpenStreetMap: OpenStreetMap database [PostgreSQL via API], © OpenStreetMap contributors. Available under the Open Database Licence from: https://openstreetmap.org. Data mining by Overpass turbo. Available at https://overpass-turbo.eu, 2021.

Patton, A., Collins, C., Naumova, E., Zamore, W., Brugge, D., and Durant, J.: An Hourly Regression Model for Ultrafine Particles in a Near-Highway Urban Area, Environmental science & technology, 48, https://doi.org/10.1021/es404838k, 2014.

Ramacher, M., Kakouri, A., Speyer, O., Steiling, J., Karl, M., Timmermans, R., Denier van der Gon, H., Kuenen, J., Gerasopoulos, E., and Athanasopoulou, E.: The UrbEm Hybrid Method to Derive High-Resolution Emissions for City-Scale Air Quality Modeling, Atmosphere, 12, 1404, https://doi.org/10.3390/atmos12111404, 2021.

Saha, P. K., Li, H. Z., Apte, J. S., Robinson, A. L., and Presto, A. A.: Urban Ultrafine Particle Exposure Assessment with Land-Use Regression: Influence of Sampling Strategy, Environmental Science & Technology, 53, 7326–7336, https://doi.org/10.1021/acs.est.9b02086, 2019.

Schmitz, O., Beelen, R., Strak, M., Hoek, G., Soenario, I., Brunekreef, B., Vaartjes, I., Dijst, M., Grobbee, D., and Karssenberg, D.: High resolution annual average air pollution concentration maps for the Netherlands, Scientific Data, 6, 190 035, https://doi.org/10.1038/sdata.2019.35, 2019.

Seibold, H., Hothorn, T., and Zeileis, A.: Detecting treatment-subgroup interactions in clustered data with generalized linear mixed-effects model trees, Advances in Data Analysis and Classification, 13, 703–725, https://doi.org/10.1007/s11634-018-0342-1, 2019.

Shairsingh, K. K., Jeong, C.-H., Wang, J. M., Brook, J. R., and Evans, G. J.: Urban land use regression models: can temporal deconvolution of traffic pollution measurements extend the urban LUR to suburban areas?, Atmospheric Environment, 196, 143–151, https://doi.org/https://doi.org/10.1016/j.atmosenv.2018.10.013, 2019.

Shi, T., Hu, Y., Liu, M., Li, C., Zhang, C., and Liu, C.: Land use regression modelling of PM2.5 spatial variations in different seasons in urban areas, Science of The Total Environment, 743, 140 744, https://doi.org/10.1016/j.scitotenv.2020.140744, 2020.

Snoun, H., Krichen, M., and Chérif, H.: A comprehensive review of Gaussian atmospheric dispersion models: current usage and future perspectives, Euro-Mediterranean Journal for Environmental Integration, 8, 219–242, 2023.

Stedman, J. R., Vincent, K. J., Campbell, G. W., Goodwin, J. W., and Downing, C. E.: New high resolution maps of estimated background ambient NOx and NO2 concentrations in the U.K., Atmospheric Environment, 31, 3591–3602, https://doi.org/https://doi.org/10.1016/S1352-2310(97)00159-3, 1997.

Taheri Shahraiyni, H. and Sodoudi, S.: Statistical Modeling Approaches for PM10 Prediction in Urban Areas; A Review of 21st-Century Studies, Atmosphere, 7, https://doi.org/10.3390/atmos7020015, 2016.

Van den Bossche, J., Peters, J., Verwaeren, J., Botteldooren, D., Theunis, J., and De Baets, B.: Mobile monitoring for mapping spatial variation in urban air quality: Development and validation of a methodology based on an extensive dataset, Atmospheric Environment, 105, 148–161, 2015.

Van den Hove, A., Verwaeren, J., Van den Bossche, J., Theunis, J., and De Baets, B.: Development of a land use regression model for black carbon using mobile monitoring data and its application to pollution-avoiding routing, Environmental Research, 183, 108 619, 2020.

van Nunen, E., Vermeulen, R., Tsai, M.-Y., Probst-Hensch, N., Ineichen, A., Imboden, M., Naccarati, A., Tarallo, S., Raffaele, D., Ranzi, A., Nieuwenhuijsen, M., Jarvis, D., Amaral, A. F., Vlaanderen, J., Meliefste, K., Brunekreef, B., Vineis, P., Gulliver, J., and Hoek, G.:

https://doi.org/10.5194/egusphere-2024-2930
Preprint. Discussion started: 20 November 2024

Associations between modeled residential outdoor and measured personal exposure to ultrafine particles in four European study areas, Atmospheric Environment, 226, 117 353, https://doi.org/https://doi.org/10.1016/j.atmosenv.2020.117353, 2020.

Wallek, S., Langner, M., Schubert, S., and Schneider, C.: Modelling Hourly Particulate Matter (PM10) Concentrations at High Spatial Resolution in Germany Using Land Use Regression and Open Data, Atmosphere, 13, https://doi.org/10.3390/atmos13081282, 2022.

Wei, J., Li, Z., Li, K., Dickerson, R. R., Pinker, R. T., Wang, J., Liu, X., Sun, L., Xue, W., and Cribb, M.: Full-coverage mapping and spatiotemporal variations of ground-level ozone (O3) pollution from 2013 to 2020 across China, Remote Sensing of Environment, 270, 112 775, https://doi.org/https://doi.org/10.1016/j.rse.2021.112775, 2022.

Wu, Y., Li, R., Cui, L., Meng, Y., Cheng, H., and Fu, H.: The high-resolution estimation of sulfur dioxide (SO2) concentration, health effect and monetary costs in Beijing, Chemosphere, 241, 125 031, https://doi.org/10.1016/j.chemosphere.2019.125031, 2019.

Xu, X., Qin, N., Qi, L., Zou, B., Cao, S., Zhang, K., Yang, Z., Liu, Y., Zhang, Y., and Duan, X.: Development of season-dependent land use regression models to estimate BC and PM1 exposure, Science of The Total Environment, 793, 148 540, https://doi.org/10.1016/j.scitotenv.2021.148540, 2021.

Yuan, Z., Kerckhoffs, J., Shen, Y., Hoogh, K. d., Hoek, G., and Vermeulen, R.: Integrating large-scale stationary and local mobile measurements to estimate hyperlocal long-term air pollution using transfer learning methods, Environmental Research, 228, 115 836, https://doi.org/10.1016/j.envres.2023.115836, 2023.

Zapata-Marin, S., Schmidt, A. M., Crouse, D., Ho, V., Labrèche, F., Lavigne, E., Parent, M.-E., and Goldberg, M. S.: Spatial modeling of ambient concentrations of volatile organic compounds in Montreal, Canada, Environmental Epidemiology, 6, e226, https://doi.org/https://doi.org/10.1097/EE9.0000000000000226, 2022.

Zhang, L., Tian, X., Zhao, Y., Liu, L., Li, Z., Tao, L., Wang, X., Guo, X., and Luo, Y.: Application of nonlinear land use regression models for ambient air pollutants and air quality index, Atmospheric Pollution Research, 12, 101 186, 2021.

Zhao, Z., Jing, Y., Luo, X.-S., and Li, Hanhan andTang, M.: Overview and Research Progresses in Chemical Speciation and In Vitro Bioaccessibility Analyses of Airborne Particulate Trace Metals, Current Pollution Reports, 7, 540–548, https://doi.org/10.1007/s40726-021-00200-9, 2021.